



Preparation of multi-walled carbon nanotube-doped TiO₂ composite and its application in petroleum refinery wastewater treatment

F. Shahrezaei^a, P. Pakravan^b, A. Hemati Azandaryani^{c,d,*}, M. Pirsaeheb^e,
A.M. Mansouri^{e,f,*}

^aAcademic Center for Education, Culture & Research (ACECR), Kermanshah, Iran, Tel. +98 9188334300;
email: fatemehshahrezai@yahoo.com

^bDepartment of Chemistry, Zanzan Branch, Islamic Azad University, Zanzan, Iran, Tel. +98 9127410459;
email: pakravanparvaneh@yahoo.com

^cNano Drug Delivery Research Center, Kermanshah University of Medical Sciences, Kermanshah, Iran, Tel. +98 9183524611;
email: hemati_abbas@yahoo.com

^dFaculty of Chemistry, Department of Applied Chemistry, Razi University, Kermanshah, Iran

^eResearch Center for Environmental Determination of Health (RCEDH), Kermanshah University of Medical Sciences, Kermanshah, Iran, Tel. +98 9123446880; email: mpirsaeheb@yahoo.com (M. Pirsaeheb), Tel. +98 9183524611; email: ammansouri34@yahoo.com (A.M. Mansouri)

^fFaculty of Chemistry, Department of Analytical Chemistry, Razi University, Kermanshah, Iran

Received 30 August 2014; Accepted 19 June 2015

ABSTRACT

Electron–hole recombination is the most important factor limiting the efficiency of TiO₂-based photocatalysts. In this work, multi-walled carbon nanotube (MWCNT) was used to suppress the electron–hole recombination and enhance the photocatalytic efficiency of titanium dioxide (TiO₂) nanoparticles. Primarily, nanocomposite of MWCNT/TiO₂ as a hybrid photocatalyst with different weight ratio of TiO₂ and MWCNT (from 0.95:0.05 to 0.75:0.25) was produced and characterized. The composites were characterized by a series of analytical techniques including SEM, TEM, XRD, and UV–vis to reveal the textural, crystallographic, and optical properties of the composites. These techniques indicated a uniform, mesoporous, and well-defined nanometer scale anatase titania (TiO₂) layer on individual MWCNT. Secondly, significantly enhanced photocatalytic activity of TiO₂ was systematically studied by introducing MWCNT in the photocatalytic oxidation and mineralization of petroleum refinery wastewater (PRW) in a batch circulating photocatalytic reactor. The results showed that when the proportion ratio of TiO₂ and MWCNT reached 0.8:0.2, the synthesized MWCNT/TiO₂ nanocomposite demonstrated the maximum photocatalytic efficiency on PRW treatment. The increase in the removal efficiency with increase in MWCNT/TiO₂ ratio was due to great capability of MWCNT in the adsorption of organic molecules and charge separation.

Keywords: Multi-walled carbon nanotube; Petroleum refinery wastewater; Wastewater treatment; TiO₂

*Corresponding authors.

1. Introduction

The rapid development of industrialization, besides its benefits, has given rise to certain hazardous effects on environment and human survival. Wastewater generated from pesticides, textile, petrochemical, dyeing, plastic, and paper industries is highly toxic, carcinogenic, and recalcitrant [1], and yet not freely degradable. Thus, these hazardous liquids must be collected and treated before discharge to the environment to satisfy the discharge standards for its variable composition and high proportion of refractory materials.

Wastewater from petroleum refinery has the characteristics of high concentration of aliphatic and aromatic petroleum hydrocarbons, which could lead to heavy pollution on the surface of soil and rivers. The quantity and quality of pollutions in the wastewater depend on the process configuration. Refineries generate polluted wastewater containing phenol, benzene, chrome, nutrients, lead, and other pollutants. Phenol and phenolic derivatives in the petroleum refinery effluents pose a significant threat to the environment due to their extreme toxicity, stability, poor biodegradability, and ability to remain in the environment for long time [2–4]. So, there is an urgent need to develop efficient and economical methods to remove these pollutants from petroleum refinery wastewater (PRW) [2].

In recent years, many strategies have been devised to remove these pollutants, such as biological oxidation, advanced oxidation processes, chemical, and physical methods [5,6]. However, these traditional methods are often costly and may cause secondary pollution; thus their implementation unfeasible under industrial conditions. Therefore, more efficient and economic methods need to be developed [7].

Besides these methods, the initial discovery of photoelectrochemical water splitting on titanium dioxide (TiO_2) electrodes by Fujishima and Honda [8] opened a new area in the destruction of organic pollutions. Photocatalytic oxidation is an alternative means for pollutant treatment in air and in water, hence heterogeneous photocatalysis by semiconductors has attracted much more attention [2,9].

The coupling of carbon nanotubes (CNTs) and TiO_2 has attracted much attention in the literature for enhanced photo-induced catalysis of ecological and renewable energy applications such as photocatalysis, photo-electro-catalysis, and CO_2 photoreduction [10–13]. Combining CNTs with TiO_2 at the nanoscale level can endorse the separation of the generated electron–hole charges. However, it was demonstrated that charge separation ability depends on the contact

between CNTs and TiO_2 , the morphological and surface properties of the nanoparticles [14,15].

Furthermore, CNTs can provide spatial confinement of TiO_2 and large supporting surface areas, leading to faster observed rates of redox reactions. Many investigations have focused on the material and photocatalytic/photo-electro-catalytic properties of heterogeneous nonuniform coatings of TiO_2 onto CNT. However, it is well known that the charge separation capability depends on both the quality of the interfacial contact between CNTs and TiO_2 and also the morphological and surface properties of the nanocomposites. Hence, tailored uniform core–shell coatings of TiO_2 on the CNTs surface should improve the transfer of photo-induced free electrons from the TiO_2 matrix to the CNTs and inhibit the recombination of photo-induced carriers through the formation of hetero junctions. Core–shell structures of a semiconductor with small and uniform thickness hindered electron–hole recombination [7,16]. As well as the probability of electron–hole recombination depends on the thickness of the oxide layer over the entire length of the composite tubes. Some uniform coatings methods have been investigated for the nanocomposite preparation such as chemical vapor deposition, electrospinning, and modified sol–gel methods [17].

Based on the best knowledge, there are few studies for photocatalytic oxidation and mineralization of PRW by multi-walled carbon nanotube (MWCNT)/ TiO_2 nanocomposite. Unlike the previous studies, the present work investigated removal of chemical oxygen demand (COD) from real PRW. In addition, in the present study, in order to explore the best operational conditions achieving high COD removal efficiency, the effects of initial nanocomposite concentration, TiO_2 :MWCNT ratio, pH, and UV and visible light irradiation on the performance of process were investigated.

2. Experimental

2.1. Materials

PRW obtained from Petroleum Company in Kermanshah Iran. CNTs (multi-walled CNTs) were purchased from Aldrich and used as received (Sigma, St. Louis, MO, USA). TiO_2 nanopowder with the average size of 25 nm and absolute ethanol was obtained from Merck Co. (Darmstadt, Germany).

The laboratory tests were accomplished using the pretreated wastewater (after flotation and coagulation). PRW samples were haphazardly collected from an oil refinery plant located in the city of Kermanshah,

Iran. The COD of the PRW sample was about 800 mg/l. The concentrations of COD were characterized by means of standard methods.

2.2. MWCNT/TiO₂ nanocomposite preparation

As a support, MWCNTs were combined with TiO₂ through sonochemical and calcination methods. To synthesize the TiO₂/MWCNTs composite, titanium oxide was used as a titanium source. Firstly, MWCNTs were sonicated in 20 mL ethanol for 30 min to properly disperse them. Then, each mixture of TiO₂ and MWCNTs, with a different weight ratio of titanium and carbon, was sonicated for 30 min to improve the interaction between the two chemicals. After adding 80-mL Milli-Q water, the sol samples formed by the hydrolysis process were treated with ultrasonic irradiation in an ultrasonic cleaning bath for another 45 min, followed by aging at 25°C over night in order to further hydrolyze the TiO₂ and form mono-dispersed TiO₂ particles. These samples were then dried and the mixtures were calcinated in a 500°C for 1 h, and the nanocomposites were obtained with the color from white gray to black, when increasing the amount of CNTs.

2.3. Nanocomposites characterization

X-ray diffraction (XRD) patterns of samples were recorded using EQUINOX diffractometer (Inel Company) operating with a Cu anode and a sealed X-ray tube at room operated at a voltage of 35 kV, current 20 mA. The 2θ scans were recorded at several resolutions using CuKα radiation of wavelength 1.548 Å in the range of 20–80 with 0.05 step size.

A surface morphology of MWCNT/TiO₂ thin films was studied by scanning electron microscopy (SEM) using a Philips XL30 microscope at an accelerating voltage of 20 kV. After oven drying of the thin film for 12 h, the sample was coated with a platinum layer using an SCDOOS sputter coater (BAL-TEC, Sweden) in an argon atmosphere. Subsequently, the sample was scanned and photomicrographs were obtained. Also, the surface properties of MWCNT/TiO₂ nanocomposite were visualized using a transmission electron microscope (TEM) (Zeiss-EM 10C-Germany) at an accelerating voltage of 80 kV capable of point-to-point transmission. The Raman spectra were recorded from 100 to 4,000 cm⁻¹ at room temperature using Almega Thermo Nicolet Dispersive Raman Spectrometer with an excitation wavelength of 532 nm of a Nd:YLF laser with laser power of 30 mW.

2.4. Photoreactor configuration

The photocatalytic activities of the composite catalysts were assessed by the degradation of PRW in a photoreactor. The photoreactor was equipped with thin gap annular photocatalytic reactor (total liquid volume of photoreactor was 950 mL excluding volume of the quartz tube (40 tubes in each of reactor) inside the photoreactor). The UV lamps (22 cm body length and 16 cm arc length) were mercury 400 W (200–550 nm) lamps. The UV lamp was fixed in the inner quartz tube of each reactor and was totally immersed in the reactor. At first, PRW flow flowed through annular reactor by means of peristaltic pump from the wastewater reservoir and subsequently discharged to the settling tank. This photoreactor was operated under room temperature (25 ± 2°C). The air was presented into the reactor with a bubble air diffuser at the bottom of the each reactor, and the air flow rate was controlled with an air flow meter connected to the blower. During reaction, 10 mL of mixed solution was withdrawn periodically from the reactor, followed by centrifugation and filtration, and the obtained clear solution was analyzed using UV spectroscopy (756CRT).

The degradation rate of petroleum refinery was calculated by the equation $d\% = (C_0 - C)/C_0\%$, where C_0 stands for the initial concentration of petroleum refinery solution, and C , at any other time [18].

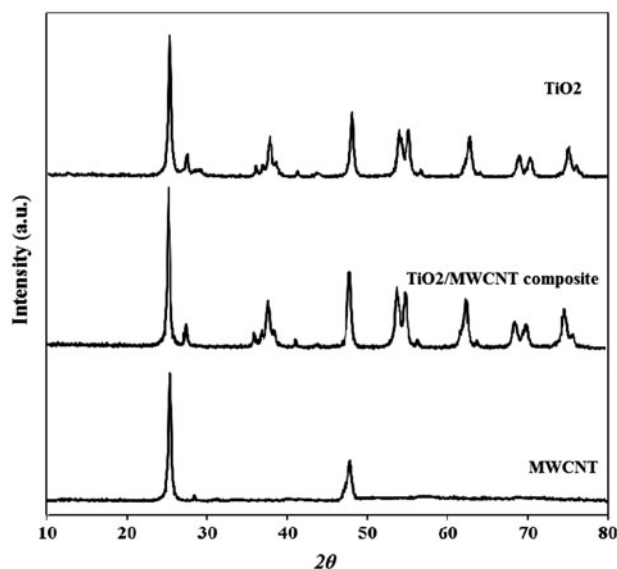


Fig. 1. XRD patterns of TiO₂, MWCNT, and TiO₂/MWCNTs composites.

3. Results and discussion

3.1. Morphological analysis

To characterize the crystalline structure of the samples, the XRD patterns of TiO_2 and $\text{TiO}_2/\text{MWCNTs}$ composites were obtained. Fig. 1 shows the XRD patterns of several samples including MWCNTs, TiO_2 , and $\text{MWCNTs}/\text{TiO}_2$, indicating that the MWCNTs sample clearly displays a primary peak at around 25.9° , which can be indexed to the reflection (0.02) of graphite and the next peak at ca. 48.5° corresponding to the (1.00) plane of graphite. In agreement with the reported results in the literature, the pattern of the titanium oxide nanopowder sample exhibits several characteristic peaks of anatase phase of TiO_2 at 25.2° , 37.7° , 48° , and 54° . For the $\text{MWCNTs}/\text{TiO}_2$ (0.10)-450 composite, the diffraction peaks assigned to the anatase phase of TiO_2 and diffraction peaks relating to MWCNTs can hardly be identified (Fig. 1). This phenomenon may be caused by the overlap of the main peak of MWCNTs at 25.9° with the main peak of anatase TiO_2 nanotubes at 25.2° [7]. Moreover, the crystalline extent of MWCNTs is much lower than that of TiO_2 , leading to the shielding of the peaks of MWCNTs by those of TiO_2 [19,20].

The SEM images of the samples are shown in Fig. 2. All samples have pores in their structures, which are connected randomly and lack discernible long-range order in the pore arrangement. It is also found that the morphology of TiO_2 changes from spherical particles to big agglomerated particles. MWCNTs have an effect on the agglomerated morphology of TiO_2 . Meanwhile, the agglomeration of mono-dispersed TiO_2 particles can be clearly observed in the SEM and TEM images with a higher resolution.

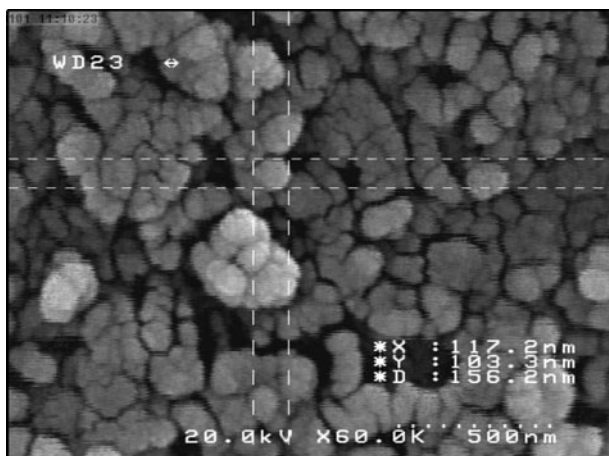


Fig. 2. SEM images of $\text{TiO}_2/\text{MWCNTs}$ composites.

The spherical TiO_2 particles with the size of about 40 nm were composed of the nanoparticles with the diameter of about 10 nm, which is basically in accordance with the crystalline size calculated from their XRD patterns [20].

It can be seen from the TEM images Fig. 3 that a uniform shell of TiO_2 with a nanoscale thickness and surface of MWCNT forms a core-shell structure. The dark and bright regions correspond to the TiO_2 and the MWCNT shell, respectively. This phenomenon can be due to their different electron-absorbing abilities, i.e. the electron binding ability of TiO_2 is higher than that of carbon. Therefore, the TiO_2 can be identified as the darker region compared to MWCNTs.

Raman spectroscopy is an effective tool to explore and describe carbonaceous materials. Fig. 4 illustrates the Raman spectra of the MWCNTs and $\text{MWCNTs}/\text{TiO}_2$ composite, showing that the two spectra exhibit several peaks positioned at around 150, 513, 635, 1,350, 1,587, and $2,700\text{ cm}^{-1}$. These diffraction peaks

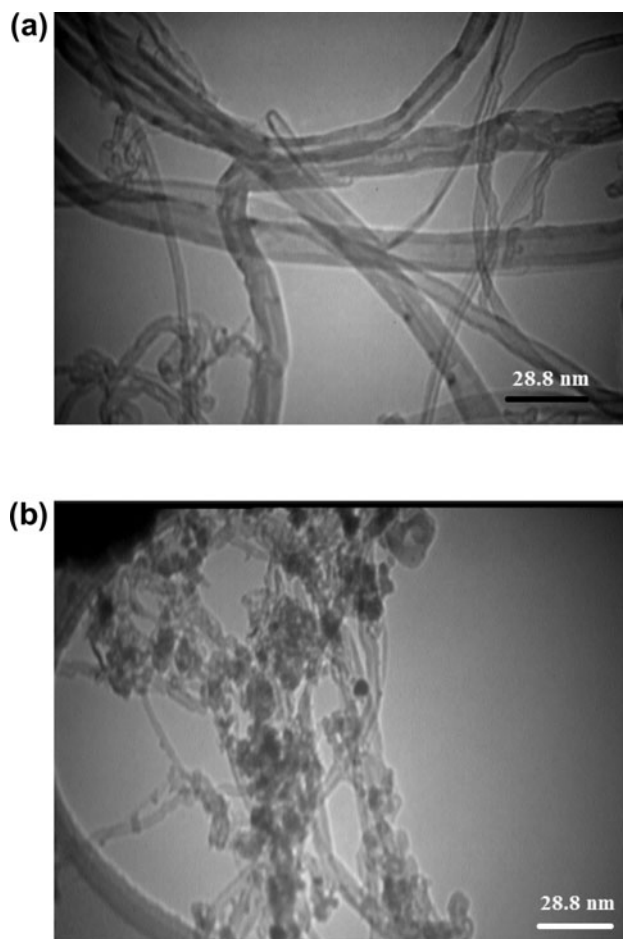


Fig. 3. TEM images of MWCNT (a) and $\text{TiO}_2/\text{MWCNTs}$ composites (b).

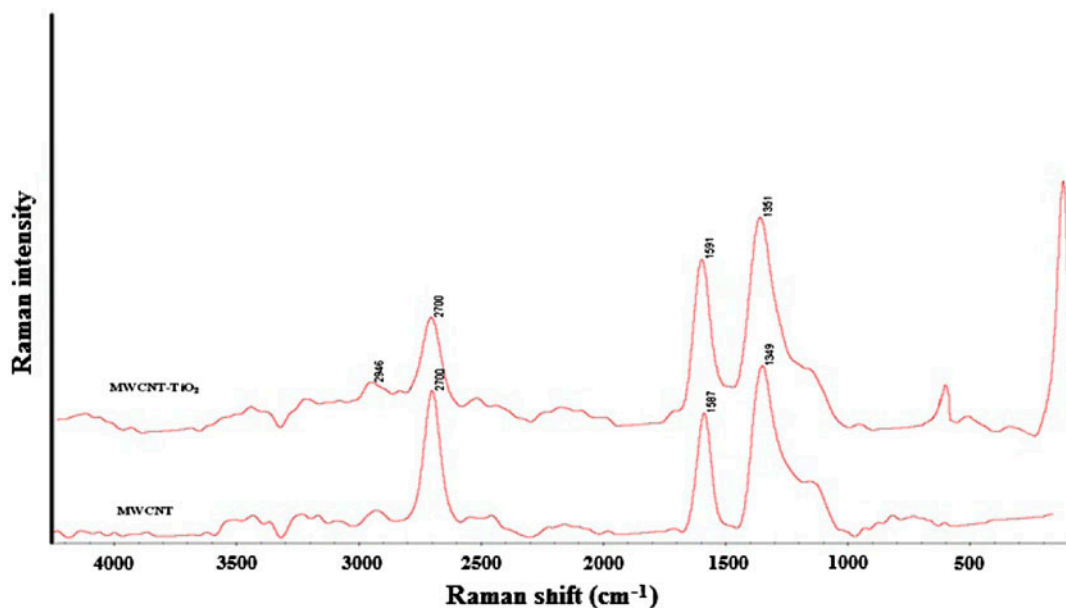


Fig. 4. Raman spectra of samples.

are designated as the characteristic peaks of MWCNTs and nanocomposite that the two characteristic peaks correspond to the typical characteristic bands of the Raman spectrum of multi-walled CNTs, located at 1,349 and 1,587 cm^{-1} , which correspond to the well-documented D band and G band, respectively. The broad peak at around 1,600 cm^{-1} is an unresolved Raman triplet identified with tangential carbon atom displacement modes, which is related to the E_{2g} mode in graphite at 1,582 cm^{-1} [20]. Also, a well-resolved TiO_2 Raman peak is observed at about 145 cm^{-1} for TiO_2 and the bonding $\text{TiO}_2/\text{MWCNT}$ composite, which is attributed to the main E_g anatase vibration mode [7,21]. These results proved that the MWCNTs/ TiO_2 composite has both the characteristic peaks of TiO_2 and the characteristic bands of MWCNTs.

3.2. Photocatalytic activity

Here, the photocatalytic activity of the composites with high MWCNTs content is much higher. Photocatalytic activity of TiO_2 may be explained by the UV–vis absorbance spectra of the samples of TiO_2 and the nanocomposite (Fig. 5). It is found that with the addition of the MWCNTs to the TiO_2 nanoparticles the absorption of UV light by the composites decreases greatly and it is shift to visible absorption. The color of MWCNTs is black so that they can shield the UV light for the absorption by TiO_2 to visible light. For a photocatalyst, light absorption is the most critical factor [20].

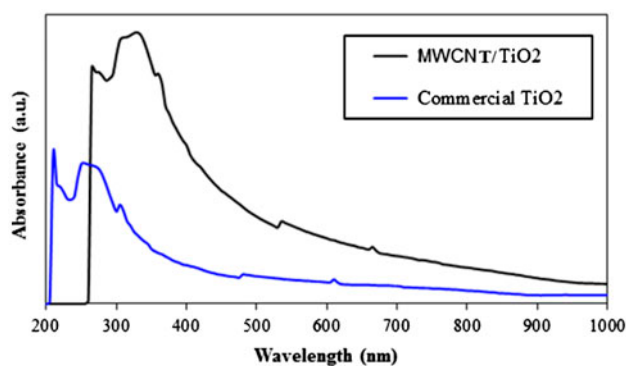


Fig. 5. UV–vis spectra of the samples of TiO_2 and MWCN/ TiO_2 nanocomposite.

This bonding $\text{TiO}_2/\text{MWCNT}$ composite should possess better photocatalytic activity than that of pure TiO_2 and the physical mixture of $\text{TiO}_2 + \text{MWCNT}$ due to the formation of chemical bond, which can enhance the electron injection into MWCNT, and thus promote their separation for electron–hole pairs.

The photocatalytic activity of the bonding $\text{TiO}_2/\text{MWCNT}$ composite toward the degradation of pollutant was investigated in different conditions in order to demonstrate the intricate correlation between structure and property, and the results are shown in Fig. 6. After UV irradiation for 120 min, as for pure TiO_2 in UV light and visible light, the degradation ratio in UV condition is much higher (Fig. 6(a)).

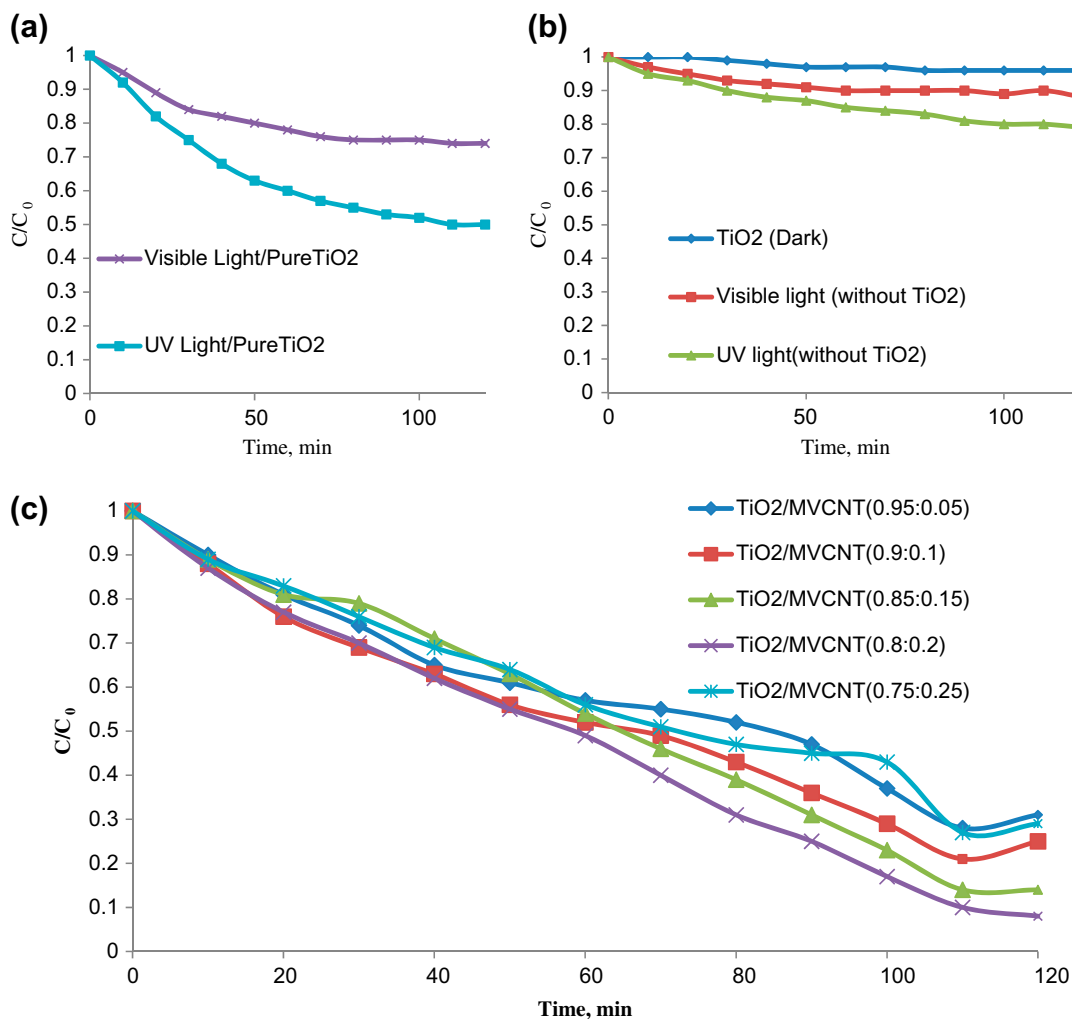


Fig. 6. Photocatalytic activity of TiO₂ nanoparticles in different condition: pure nano TiO₂ in visible and UV light (a), degradation of pollutant in different condition (b), the effect of amount of MWCNT in degradation of pollutant.

Fig. 6(b) shows the existing effect of nano TiO₂ on the degradation, and it was shown that the TiO₂ and light must exist with each other for pollutant degradation. Fig. 6(c) demonstrated the effect of MWCNT on the photocatalytic activity of nanocomposite. From this figure it was shown that an increase in the carbon enhanced the effectivity of nano TiO₂. This increase in the photocatalytic activity is relative to the formation of chemical bond between TiO₂ and MWCNT (the formation of ester bond), and their large surface area (as Zhou et al. obtained the 171 m² g⁻¹ for this value) because MWCNT could also act as a disperser and supporter of TiO₂ for obtaining large surface area [21,22]. Also, at the interface, electrons will flow from the higher to lower Fermi level material to align the Fermi energy levels. In general, CNT is composed of one-third metal and two-third semiconductor ones.

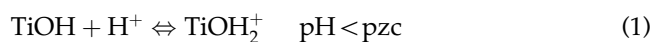
The formation of ester bonds resulting from a close contact between TiO₂ and MWCNT will form a Schottky barrier. Therefore, the TiO₂/MWCNT Schottky barrier junction offers an effective route of decreasing recombination of photogenerated electron-hole pairs. In this work, the photocatalytic activity of the composites with varying MWCNT content was also investigated. While the MWCNT was too little or too much, the photocatalytic activities were poor. If the MWCNT was too little, not too much ester bonds can be formed and thus not in favor of separating electron-hole pairs. On the contrary, if they were too much, residual MWCNT, which could not form ester bond, play only the role of adsorption, thus weaken the activity of TiO₂ and decrease the photocatalytic activity. Therefore, the content of MWCNT in this bonding composite must be moderate [23].

As summarized in Zhou and co-workers literature [21] about this phenomenon, two things could be presented also in our study: (1) The formation of ester bond improved the interface of TiO₂ and MWCNT, reduced the distance between TiO₂ and SWCNT; thus it favored the injection of electrons into MWCNT and inhibited the recombination of photogenerated electron–hole pairs. (2) Large surface area resulted in excellent adsorption performance and offered adequate active sites to participate in photocatalysis. Moreover, due to the compact contact between them and MWCNT, some electrons can be deposited, photo-generated carriers can be effectively separated. All the above mentioned are considered positive factors for the enhancement of photocatalytic activity.

3.3. Effect of pH on COD removal efficiency

The effect of pH on the COD removal was investigated in this study. The examination of Fig. 7 shows that the pH of the emulsion has a crucial effect on performance. As shown in Fig. 7, the amount of COD removal is decreased with an increase in pH, which is due to a repulsion between MWCNT and pollutant [2].

Interpretation of such positive and negative impacts of the pH on the COD removal efficiency in this reactor is a very difficult task in terms of many organic pollutants and intermediates, which exist in PRW. However, attempts have been made to explain this phenomenon. The pH-effect is related to the point of zero charge (pzc) of TiO₂ at pH 6.2 and charge of organic matters in different pH [24]. In acidic media (pH < 6.2), the surface of TiO₂ is positively charged, whereas it is negatively charged under alkaline conditions (pH > 6.2) according to Eqs. (1) and (2).



Since the majority of organic matters in PRW is phenol and phenolic derivatives are negatively charged due to the OH groups ionized in water, their electrostatic attraction to the TiO₂ surface is favorable in acidic solution and forbidden in alkaline media due to the coulombic repulsion between the negatively charged surface of TiO₂ and the organic molecules. Thus, the reaction rate reached a maximum value at very low pH. Moreover, the generation of OH radicals by the effect of UV light on the TiO₂ of the composite may also represent a further factor for increasing reaction rate in acidic environment [25].

3.4. Effect of initial nanocomposite concentration on COD removal efficiency

Fig. 8 showed the effect of MWCNT/TiO₂ concentration in the pH of 3 on the COD removal. As shown in this figure, the COD removing is increased with an increase in the concentration from 2 to 10 g/L, but with the concentration enhancing from 10 to 15 g/L the COD removing is decreased, which is due to the aggregation of nanocomposite in high concentration. Also, the UV transmission from solution is decreased with an increase in the concentration, which would have negative effect on the COD removal.

In order to identify the present of hazardous organic compounds in the samples and to compare the efficiency of degradation for different compounds, 5 mL of PRW-treated samples were taken before and after the degradation. The catalyst particles were

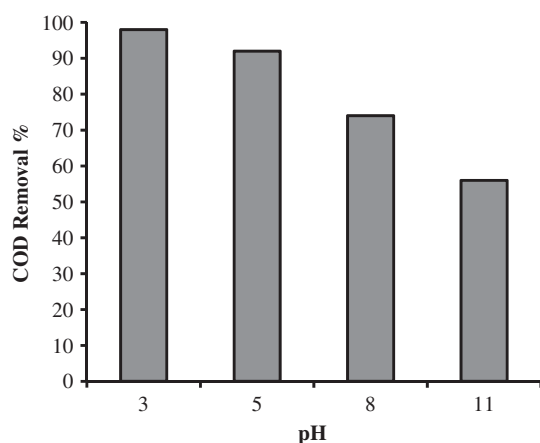


Fig. 7. Effect of pH on pollutant degradation.

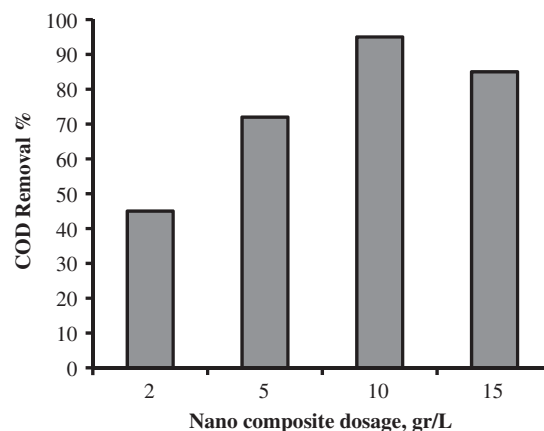


Fig. 8. Investigation of nanocomposite concentration on COD removal.

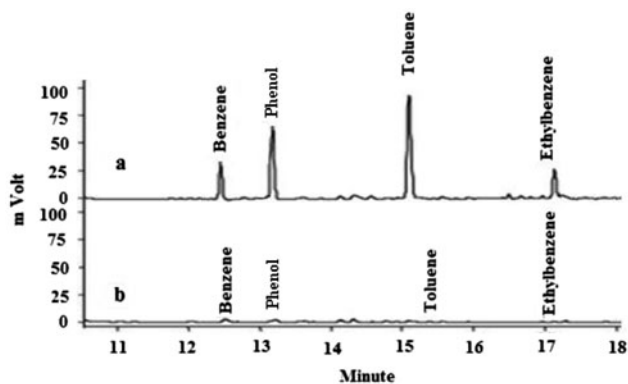


Fig. 9. Chromatograms of the analyzing wastewater, before (a) and after (b) the degradation under optimum conditions.

separated and the samples were analyzed by means of the gas chromatography (GC). Fig. 9(a) and (b) presents the chromatograms of the analyzing wastewater before and after the degradation under optimum conditions. The major peaks have been labeled by name according to the GC identification. Comparison of spectra in the figure verified that all hazardous compounds were degraded at high efficiencies.

3.5. Proposed degradation mechanism for benzene and phenol as a constituents of PRW

TiO₂ can absorb ultraviolet radiation of $\lambda \leq 413$ nm, which induces valence band electrons to the conduction band, leaving positive holes (h⁺) in the valence band. Possible reaction pathways have been given below:

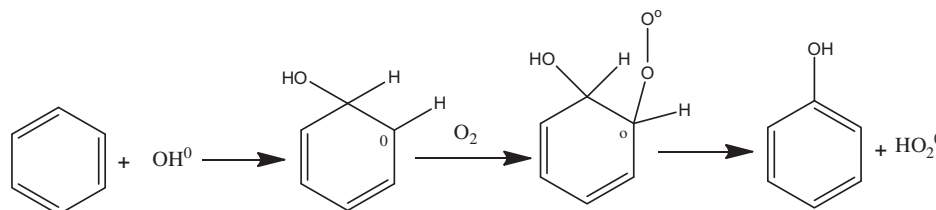


Fig. 10. Route of benzene degradation by OH⁰ radical addition.

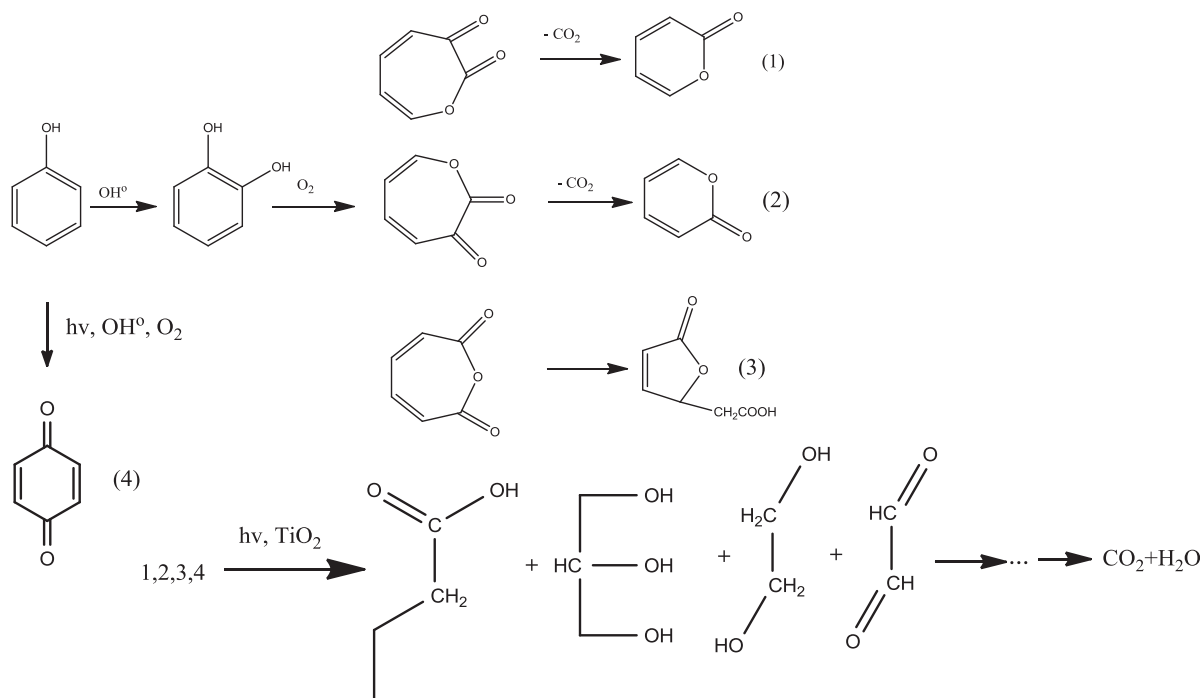


Fig. 11. Proposed degradation mechanism for phenol.



It has also been reported that benzene and toluene is destructed because of the existing hydroxyl radicals [26]. Actually, in the presence of h^+ hole, benzene altered to phenol (Fig. 10).

In general, the degradation of phenol follows the oxidation of phenol to other hydroxylated or oxygenated compounds, especially cyclic intermediates, the ring opening reaction to form organic acids, and mineralization of organic acids to carbon dioxide (Fig. 11) [26,27].

4. Conclusion

In this study, with the introduction of MWCNT to TiO_2 NPs, MWCNT/ TiO_2 nanocomposite was fabricated successfully and it shows significantly enhanced photocatalytic activity for the degradation of PRW in the presence of UV and visible light irradiation as compared to pure TiO_2 . The composites were characterized by a series of analytical techniques including SEM, TEM, XRD, and UV–vis to reveal the textural, crystallographic, and optical properties of the composites. The efficiency of photodegradation of PRW in the presence of MWCNT/ TiO_2 /UV (or visible) was investigated with changing various experimental parameters (TiO_2 :MWCNT ratio, initial nanocomposite concentration, pH, and UV and visible light irradiation). The obtained results indicated that introduction of MWCNT to TiO_2 NPs provide shorter distance for electron transfer to the TiO_2 and higher electronic conductivity of the nanocomposite catalyst that lead to control the rate of electron–hole recombination on the photocatalyst surface. Maximum COD removal from PRW (95%) was achieved at the optimum conditions (TiO_2 :MWCNT ratio of 0.8:0.2, initial nanocomposite concentration of 10 mg/l, and pH of 3).

References

- [1] S.M. Lam, J.C. Sin, A.R. Mohamed, Parameter effect on photocatalytic degradation of phenol using TiO_2 -P25/activated carbon (AC), Korean J. Chem. Eng. 27 (2010) 1109–1116.
- [2] F. Shahrezaei, Y. Mansouri, A.A. Lorestani Zinatizadeh, A. Akhbari, Process modeling and kinetic evaluation of petroleum refinery wastewater treatment in a photocatalytic reactor using TiO_2 nanoparticles, Powder Technol. 221 (2012) 203–212.
- [3] O. Abdelwahab, N.K. Amin, E.S.Z. El-Ashtouky, Electrochemical removal of phenol from oil refinery wastewater, J. Hazard. Mater. 163 (2009) 711–716.
- [4] S.K. Pardeshi, A.B. Patil, A simple route for photocatalytic degradation of phenol in aqueous zinc oxide suspension using solar energy, Solar Energy 82 (2008) 700–705.
- [5] N. Panda, H. Sahoo, S. Mohapatra, Decolourization of Methyl Orange using Fenton-like mesoporous Fe_2O_3 - SiO_2 composite, J. Hazard. Mater. 185 (2011) 359–365.
- [6] S. Jan, A.N. Kamili, T. Parween, M. Ahmad, Feasibility of radiation technology for wastewater treatment, Desalin. Water Treat. (2014) 1–16.
- [7] T. Jiang, L. Zhang, M. Ji, Q. Wang, Q. Zhao, X. Fu, H. Yin, Carbon nanotubes/ TiO_2 nanotubes composite photocatalysts for efficient degradation of Methyl Orange dye, Particuology 11 (2013) 737–742.
- [8] A. Fujishima, K. Honda, Electrochemical photolysis of water at a semiconductor electrode, Nature 238 (1972) 37–38.
- [9] X. Zhang, D.K. Wang, D.R. Schmeda Lopez, J.C.D da Costa, Fabrication of nanostructured TiO_2 hollow fiber photocatalytic membrane and application for wastewater treatment, Chem. Eng. J. 236 (2014) 314–322.
- [10] B. Ahmmad, Y. Kusumoto, S. Somekawa, M. Ikeda, Carbon nanotubes synergistically enhance photocatalytic activity of TiO_2 , Catal. Commun. 9 (2008) 1410–1413.
- [11] S. Aryal, C.K. Kim, K.W. Kim, M.S. Khil, H.Y. Kim, Multi-walled carbon nanotubes/ TiO_2 composite nanofiber by electrospinning, Mater. Sci. Eng. 28 (2008) 75–79.
- [12] C.G. Silva, J.L. Faria, Photocatalytic oxidation of benzene derivatives in aqueous suspensions: Synergic effect induced by the introduction of carbon nanotubes in a TiO_2 matrix, Appl. Catal. B: Environ. 101 (2010) 81–89.
- [13] X. Qu, P.J.J. Alvarez, Q. Li, Applications of nanotechnology in water and wastewater treatment, Water Res. 47 (2013) 3931–3946.
- [14] Z. Li, B. Gao, G.Z. Chen, R. Mokay, S. Sotiropoulos, G.L. Puma, Carbon nanotube/titanium dioxide (CNT/ TiO_2) core-shell nanocomposites with tailored shell thickness, CNT content and photocatalytic/photoelectrocatalytic properties, Applied Catal. B: Environ. 110 (2011) 50–57.
- [15] S.M. Lam, J.C. Sin, A. Zuhairi Abdullah, A.R. Mohamed, Photocatalytic TiO_2 /carbon nanotube nanocomposites for environmental applications: An overview and recent developments, fuller. Nanotub. Car. N. 22 (2014) 471–509.
- [16] P. Brown, K. Takechi, P.V. Kamat, Single-walled carbon nanotube scaffolds for dye-sensitized solar cells, J. Phys. Chem. 112 (2008) 4776–4782.
- [17] M. Barberio, V. Pingitore, P. Barone, M. Davoli, F. Stranges, F. Xua, A. Bonanno, Synthesis of carbon nanotube/ TiO_2 composites by titanium evaporation in ultra high vacuum ambient, Microelectron. Eng. 108 (2013) 213–217.
- [18] R.M. Mohamed, A.A. Ismail, I. Othman, I.A. Ibrahim, Preparation of TiO_2 -ZSM-5 zeolite for photodegradation of EDTA, J. Mol. Catal. A. 238 (2005) 151–157.
- [19] S.W. Lee, W.M. Sigmund, Formation of anatase TiO_2 nanoparticles on carbon nanotubes, Chem. Commun. 21 (2003) 780–781.

- [20] Y. Yu, J.C. Yu, J.G. Yu, Y.C. Kwok, Y.K. Che, Enhancement of photocatalytic activity of mesoporous TiO₂ by using carbon nanotubes, *Applied Catal. A* 289 (2005) 186–196.
- [21] W. Zhou, K. Pan, Y. Qu, F. Sun, C. Tian, Z. Ren, G. Tian, H. Fu, Photodegradation of organic contamination in wastewaters by bonding TiO₂/single-walled carbon nanotube composites with enhanced photocatalytic activity, *Chemosphere* 81 (2010) 555–561.
- [22] Z. Kan, M. Zeda, O. Wonchun, Degradation of rhodamine B by Fe-carbon nanotubes/TiO₂ composites under UV light in aerated solution, *Chin. J. Catal.* 31 (2010) 751–758.
- [23] Y. Luo, J. Liu, X. Xia, X. Li, T. Fang, S. Li, Q. Ren, J. Li, Z. Jia, Fabrication and characterization of TiO₂/short MWNTs with enhanced photocatalytic activity, *J. Mater. Lett.* 61 (2007) 2467–2472.
- [24] M. Pera-Titus, V. Garcia-Molina, M.A. Baños, J. Giménez, S. Esplugas, Degradation of chlorophenols by means of advanced oxidation processes: A general review, *Appl. Catal. B Environ.* 47 (2004) 219–256.
- [25] A.M. Mansouri, F. Shahrezaei, A.A.L. Zinatizadeh, A. Hemati Azandaryani, M. Pirsahab, K. Sharafi, Preparation of poly ethyleneimine (PEI)/titania (TiO₂) multilayer film on quartz tube by layer-by-layer self-assembly and its applications for petroleum refinery wastewater treatment, *J. Taiwan Inst. Chem. Eng.* 45 (2014) 2501–2510.
- [26] M. Gholami, H.R. Nassehinia, A. Jonidi-Jafari, S. Nasser, A. Esrafil, Comparison of benzene & toluene removal from synthetic polluted air with use of nano photocatalytic TiO₂/ZNO process, *J. Environ. Health Sci. Eng.* 12 (2014) 1–8.
- [27] T.S. Jamil, T.A. Gad-Allah, M.E.M. Ali, M.N.B. Momba, Utilization of nano size TiO₂ for degradation of phenol enriched water by solar photocatalytic oxidation, *Desalin. Water Treat.* 53 (2015) 1101–1106.